Upgraded millimeter-wave interferometer for measuring the electron density during the beam extraction in the negative ion source

Review of Scientific Instruments

Upgraded millimeter-wave interferometer for measuring the electron density during the beam extraction in the negative ion source

Cite as: Rev. Sci. Instrum. **87**, 11E105 (2016); https://doi.org/10.1063/1.4959841
Submitted: 02 June 2016 • Accepted: 26 June 2016 • Published Online: 14 November 2016

T. Tokuzawa, M. Kisaki, K. Nagaoka, et al.

Upgraded millimeter-wave interferometer for measuring the electron density during the beam extraction in the negative ion source

T. Tokuzawa,[1,a)] M. Kisaki,[1] K. Nagaoka,[1] K. Tsumori,[1,2] Y. Ito,[1] K. Ikeda,[1] H. Nakano,[1] M. Osakabe,[1,2] Y. Takeiri,[1,2] and O. Kaneko[3]
[1]*National Institute for Fusion Science, 322-6 Oroshi-cho, Toki 509-5292, Japan*
[2]*The Graduate University for Advanced Studies, 322-6 Oroshi-cho, Toki 509-5292, Japan*
[3]*National Institutes of Natural Sciences, 4-3-13 Toranomon, Minato-ku, Tokyo 105-0001, Japan*

(Presented 7 June 2016; received 2 June 2016; accepted 26 June 2016; published online 1 August 2016)

The upgraded millimeter-wave interferometer with the frequency of 70 GHz is installed on a large-scaled negative ion source. Measurable line-averaged electron density is from 2×10^{15} to 3×10^{18} m^{-3} in front of the plasma grid. Several improvements such as the change to shorter wavelength probing with low noise, the installation of special ordered horn antenna, the signal modulation for a high accuracy digital phase detection, the insertion of insulator, and so on, are carried out for the measurement during the beam extraction by applying high voltage. The line-averaged electron density is successfully measured and it is found that it increases linearly with the arc power and drops suddenly at the beam extraction. *Published by AIP Publishing.* [http://dx.doi.org/10.1063/1.4959841]

I. INTRODUCTION

The understanding of the dynamics of the negative ion and electron during the beam extraction in the negative ion source is important not only for the neutral beam injection (NBI) heating in magnetically confined fusion plasma but also for high-energy particle accelerator development. The negative ion current density has been increased by the several intensive efforts,[1–5] and it will become the order of 100 MW in ITER. In such a high power operation, the accelerated electrons might damage the beam line components due to the heavy heat load. Therefore, the suppression of electron components is one of the key issues for the fusion plasma application. For this aim, the electron density measurement is demanded in the dynamic range of 10^{16}-10^{18} m^{-3}. The Langmuir probe can give the information on the electron density qualitatively, but it has difficulty in obtaining the electron density precisely due to the strong magnetic field in the plasma arc chamber and the contribution of negative ions to the electron saturation current.

Previously, a 39 GHz millimeter-wave interferometer was temporarily installed in the test stand of 1/3-scaled negative ion source for the LHD-NBI system, in order to test the possibility of electron density measurement near the plasma grid (PG). This interferometer successfully measured the electron density in the pure hydrogen in the plasma arc chamber without the beam extraction voltage.[6] In order to measure the electron density with higher sensitivity during the high voltage applied operation, the millimeter-wave interferometer system needs to be modified.

The performed configuration in negative ion source[7] is shown in Fig. 1. The ion source is a cesium-seeded volume-production source. An arc chamber has dimensions of 220 mm × 350 mm in cross section and 700 mm in height, which is surrounded by a strong cusp magnetic field of 0.2 T. The external magnetic filter is generated as a transverse magnetic field in front of the PG by a pair of permanent magnet rows facing each other with a separation of 350 mm. The filter magnetic field strength is around 6 mT at the center. Two cesium ovens are attached to a back plate of the arc chamber. The most important area for negative ion production is in front of the PG. In order to observe plasma parameters and their behaviors, a diagnostic flange is installed between the arc chamber flange and the PG flange. A cavity ring-down method,[8] a spectroscopy,[9] and the Langmuir probes[7] have also been installed in this flange.

In this paper, we describe the upgraded millimeter-wave interferometer system in Section II. In this upgrade, we have changed the following: (1) the diagnostic flange width enlarges in order to make the wider space in front of the PG. The center of the diagnostic flange is 18 mm far from the PG; (2) the in-vessel launcher/receiver antennae are changed to the conical horn and the higher probing frequency is utilized, in order to make a narrower probing millimeter-wave beam shape for the reduction of interaction with the PG; (3) the higher phase sensitivity is achieved even in such a higher probing frequency; (4) the insulation against the applied high voltage of 80 kV to the negative ion source is inserted into the transmission line. Then, the experimental results are presented in Section III. Finally, in Section IV, we draw the summary.

II. MILLIMETER-WAVE INTERFEROMETER

We have constructed the super heterodyne millimeter-wave interferometer system for electron density measurements in the negative ion source as shown in Fig. 2. A microwave dielectric resonator oscillator (DRO) whose frequency is 17.5 GHz (f_0) and output power is 13 dBm is used as a probe source, because it has a low phase noise and its

Note: Contributed paper, published as part of the Proceedings of the 21st Topical Conference on High-Temperature Plasma Diagnostics, Madison, Wisconsin, USA, June 2016.

a)Author to whom correspondence should be addressed. Electronic mail: tokuzawa@nifs.ac.jp.

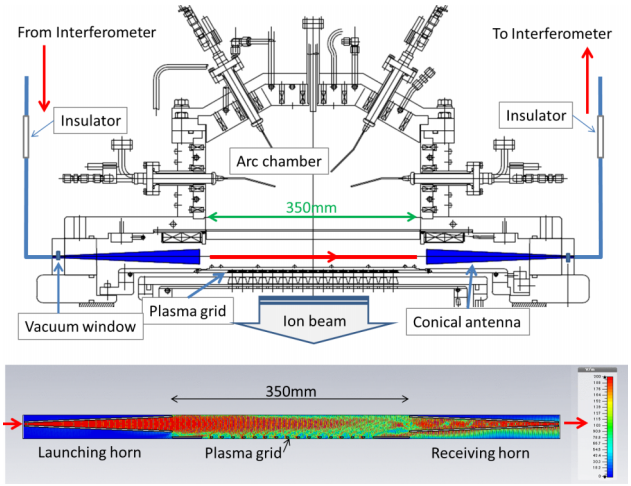

FIG. 1. Schematic of the cross section of an arc chamber (350×220 mm). The traveling path of millimeter-wave is around 350 mm and the line of sight is around 18 mm far from the plasma grid surface. In order to protect the charging when the operation of high voltage is applied to the negative ion source, the Teflon rod as an insulator is inserted into the waveguide transmission line. The bottom figure shows the calculated propagating beam pattern.

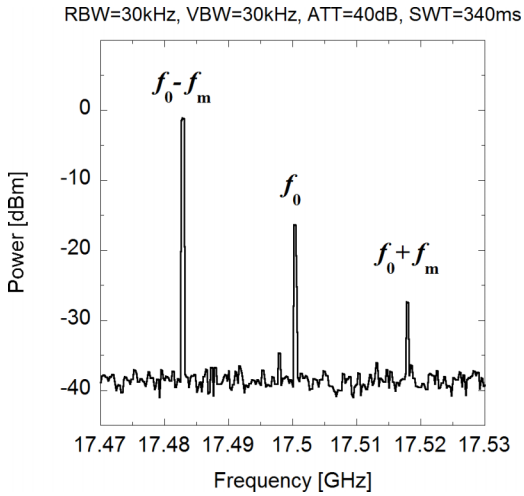

FIG. 3. Frequency spectrum of single-side-band modulating output.

harmonics are less than 40 dB. Before the plasma launching, a single-side-band (SSB) modulation is applied to the probing wave. The SSB modulator, which is driven by a 17.5 MHz (f_m) direct digital synthesizer (DDS), shifts the frequency of the reference signal for heterodyne detection. The suppression levels of the image sidebands are less than −25 dB in this system as shown in Fig. 3. For the plasma probing, the output frequency is quadrupled by the active-multiplier up to 69.930 GHz as a probe signal and 70.000 GHz as a reference signal. The probing millimeter-wave is traveling through the V-band rectangular waveguide whose total length is around 7 m and launching from the conical horn, which is installed in

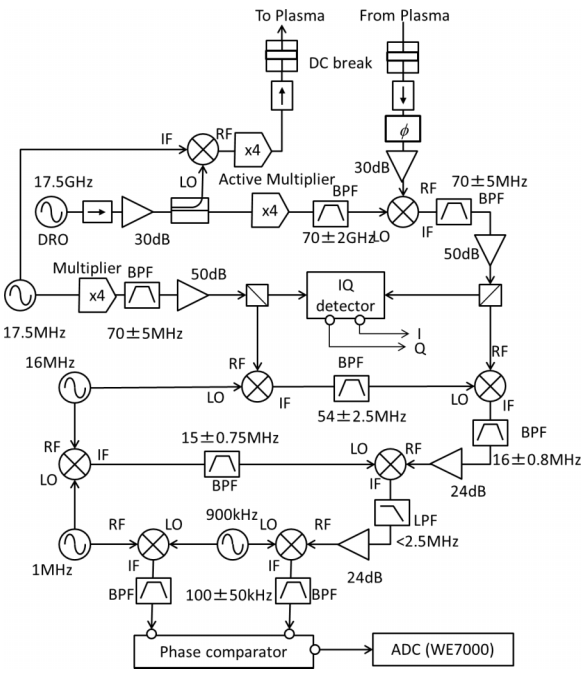

FIG. 2. Schematic of the millimeter-wave interferometer system.

the arc chamber through the vacuum window. The launching millimeter-wave passes the plasma and is received in the opposite horn. For the protection of the diagnostics system from the biased electric high voltage to the negative ion source, the electric insulator is necessary. Two Teflon rods (4 mm diameter and 250 mm length) and 100 μm Mylar sheets are used for this aim. The insulation characteristic of Teflon is 20 kV/mm and that of Mylar is 150 kV/mm. Especially, a Teflon rod is used as a dielectric waveguide. The tip of the rod is slightly sharpened and fitted into a V-band waveguide. Therefore, the insulation is sufficient in the current experiment in the negative ion source. In addition, the total transmission loss is around −30 dB including these insulators.

The receiving signal is led to the mixer and down-converted. A super heterodyne technique is adapted in order to compensate for the drift of the source frequency and promise the accurate phase measurement. Because the phase comparator outputs the phase difference between the probe and the reference signals, the stable and accurate frequency is essentially required. The intermediate frequency (IF) is at first 70 MHz, and after the multiple down-conversion by several local oscillators whose frequencies are 16.0, 1.0, and 0.9 MHz, it is finally 100 kHz. A pair of down-converted 100 kHz signals are fed to the digital phase comparator. The digital phase comparator, as shown in Fig. 4, which logic is based on the former analog phase comparator,[10,11] is utilized by the field-programmable gate array (FPGA) board (XILINX Spartan-3) for replacing from the analog phase comparing part to a time-to-digital-convert counter in this time. This digital phase comparator is driven by the internal 192 MHz clock frequency and its phase resolution is around 1/1920 fringes. The output of the phase comparator is ±5 V/fringe and the resolution of the output is around 5 mV. In the results, the resolution of line-averaged electron density is 1.5×10^{15} m^{-3}. In addition, the IQ phase detection is also available in this heterodyne system. A pair of 70 MHz IF signals are divided and led into the IQ detector. The outputs of the phase comparator and the IQ detector are acquired by the data acquisition system, for which the sampling rate is 50 kHz.

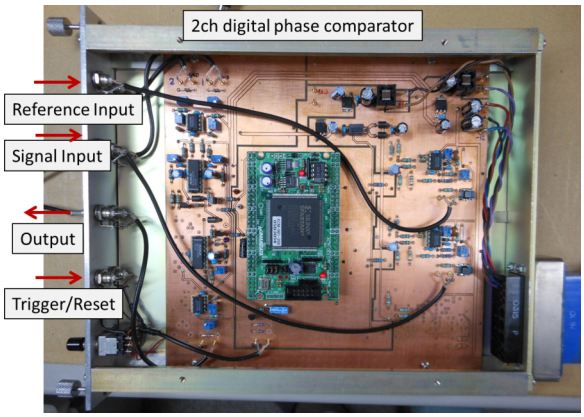

FIG. 4. Photograph of digital phase comparator.

III. EXPERIMENTAL RESULTS

The interferometer is operated to measure the line-averaged electron density during the arc discharges. The millimeter-wave can pass through the plasma in front of the PG surface. Here, the electric field of the millimeter-wave is perpendicular to the PG. The phase difference ($\Delta\phi$) between both the probe and the reference signals is expressed by

$$\Delta\phi = k_0(1-\overline{\mu})L \sim k_0\overline{n_e}L/2n_c. \quad (1)$$

Here, $\overline{\mu}$ is the line-averaged refractive index, $\overline{n_e}$ is the line-averaged electron density, L is the line of sight, and n_c is the cutoff density of the probing frequency. In the assumption of $L = 0.2$ m, the line-averaged density $\overline{n_e} = 2.6 \times 10^{18}$ m^{-3}/fringe. In addition, the direction of the magnetic field of the filter magnet in the arc chamber is parallel to the line of sight. The effect of the magnetic field is considered. In the case of the absent magnetic field, $\overline{\mu} = \left(1-\omega_{pe}^2/\omega^2\right)^{0.5}$ as an ordinary wave. In the case of the present magnetic field, $\overline{\mu_{R,L}} = \left(1-\omega_{pe}^2/\omega\left(\omega \mp \omega_{ce}\right)\right)^{0.5}$ as R-wave or L-wave. Here, ω_{pe} and ω_{ce} mean the electron plasma frequency and the cyclotron frequency, respectively. In Fig. 5(a), the estimated phase differences in three cases are plotted. Each calculated value is very close because the magnetic field strength is not so large. Figure 5(b) shows the ratio of R-wave to ordinary wave and L-wave to ordinary wave as the indicator of error. The discrepancy is less than ±0.3% and is much smaller than the system environment noise. Therefore, the line-averaged electron density is estimated by Eq. (1) in this experiment.

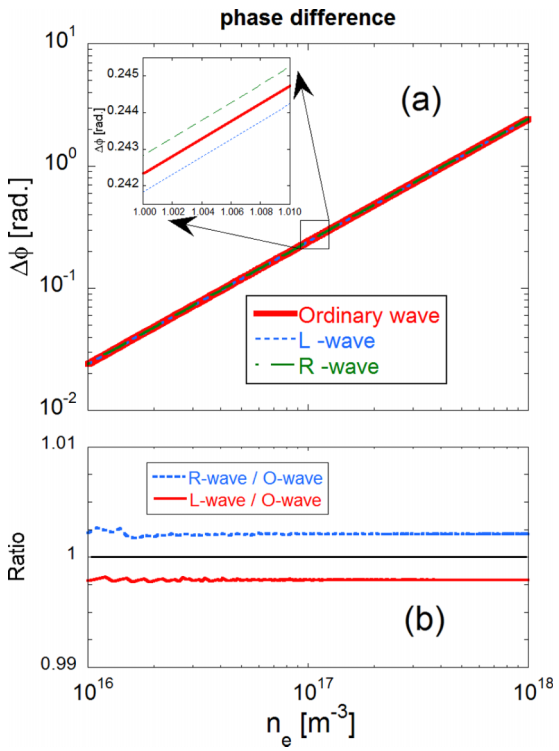

FIG. 5. (a) Calculated phase difference as a function of electron density. In each calculation, it is assumed that the polarization is ordinary mode (red solid line), L-wave (blue dotted line), and R-wave (green dashed line). (b) The ratio of R-wave and ordinary wave (blue dotted line) and that of L-wave and ordinary wave (red solid line).

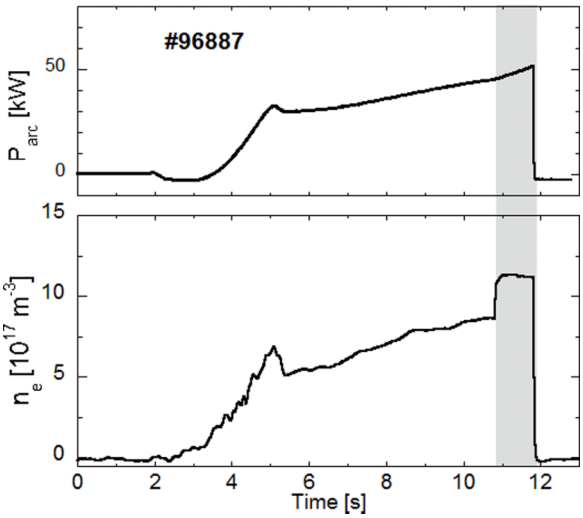

FIG. 6. Temporal behavior of the input power to arc chamber (top) and the line-averaged electron density (bottom). After $t = 10.8$ s (hatching area), high voltage is applied to extract the negative ion beam.

Figure 6 shows the typical waveform of an arc discharge. In this discharge, the arc power increases quickly and then gradually up to around 50 kW. The line-averaged electron density increases similarly to the arc power before $t = 10.8$ s. During $t = 10.8$–11.8 s, the beam extraction voltage is applied, and it is clearly found that the line-averaged electron density rapidly rises. In an earlier experiment, the negative ion density has shown a different response to the extraction voltage and has rapidly fallen.[12] Therefore, we can now analyze the negative ion density ratio $R(= n_{H^-}/(n_e + n_{H^-}))$ with high accuracy.

IV. SUMMARY

The upgraded millimeter-wave interferometer is installed in 1/3-scaled negative ion source of LHD-NBI system to measure the electron density near the plasma grid during the negative ion beam extracting condition. The probing frequency is up to 70 GHz and the super-heterodyne phase detection system is constructed by using an SSB modulation technique. The probing millimeter-wave beam shape is improved by the in-vessel conical horn antenna and wider diagnostic flange. The electrical insulator against the high voltage applied to the

negative ion source can protect the diagnostic system. The high phase resolution of 1/1920 fringe is achieved by using a digital phase comparator. Then, the line-averaged electron density is successfully obtained by the upgraded interferometer system.

ACKNOWLEDGMENTS

The authors thank the technical staff of LHD-NBI group for excellent operation of NBI test stand. The present study was partially supported by KAKENHI (Nos. 26630474, 25289342, and 25249134) and performed with the support and under the auspices of the NIFS Collaboration Research Program.

[1]Y. Takeiri, O. Kaneko, K. Tsumori, M. Osakabe, K. Ikeda, K. Nagaoka, H. Nakano, E. Asano, T. Kondo, M. Sato, M. Shibuya, S. Komada, and LHD Experiment Group, Fusion Sci. Technol. **58**, 482 (2010).
[2]K. Tsumori, Y. Takeiri, O. Kaneko, M. Osakabe, A. Ando, K. Ikeda, K. Nagaoka, H. Nakano, E. Asano, M. Shibuya, M. Sato, T. Kondo, and M. and komada, Fusion Sci. Technol. **58**, 489 (2010).
[3]H. Tobari, T. Seki, N. Takado, M. Hanada, T. Inoue, M. Kashiwagi, A. Hatayama, and K. Sakamoto, Plasma Fusion Res. **2**, 22 (2007).
[4]K. Ikeda, Y. Takeiri, O. Kaneko, K. Nagaoka, Y. Oka, M. Osakabe, K. Tsumori, M. Sato, E. Asano, and T. Kawamoto, Rev. Sci.Instrum. **75**, 1744 (2004).
[5]M. Hanada, T. Seki, N. Takado, T. Inoue, T. Mizuno, A. Hatayama, M. Kashiwagi, K. Sakamoto, M. Taniguchi, and K. Watanabe, Nucl. Fusion **46**, S318 (2006).
[6]K. Nagaoka, T. Tokuzawa, K. Tsumori, H. Nakano, M. Osakabe, K. Ikeda, M. Kisaki, Y. Takeiri, O. Kaneko, and NBI Group, AIP Conf. Proc. **1390**, 374 (2011).
[7]K. Tsumori, H. Nakano, M. Kisaki, K. Ikeda, K. Nagaoka, M. Osakabe, Y. Takeiri, O. Kaneko, M. Shibuya, E. Asano, T. Kondo, M. Sato, S. Komada, H. Sekiguchi, N. Kameyama, T. Fukuyama, S. Wada, and A. Hatayama, Rev. Sci. Instrum. **83**, 02B116 (2012).
[8]H. Nakano, K. Tsumori, K. Ikeda, K. Nagaoka, M. Kisaki, U. Fantz, M. Osakabe, O. Kaneko, E. Asano, T. Kondo, M. Sato, M. Shibuya, S. Komada, H. Sekiguchi, and Y. Takeiri, AIP Conf. Proc. **1390**, 359 (2011).
[9]K. Ikeda, K. Nagaoka, Y. Takeiri, U. Fantz, O. Kaneko, M. Osakabe, Y. Oka, and K. Tsumori, Rev. Sci. Instrum. **79**, 02A518 (2008).
[10]K. Kawahata, K. Tanaka, Y. Ito, A. Ejiri, and R. J. Wylde, Rev. Sci. Instrum. **70**, 695 (1999).
[11]Y. Ito, K. Tanaka, T. Tokuzawa, T. Akiyama, S. Okajima, and K. Kawahata, Fusion Eng. Des. **74**, 847 (2005).
[12]K. Ikeda, S. Geng, K. Tsumori, H. Nakano, M. Kisaki, K. Nagaoka, M. Osakabe, O. Kaneko, and Y. Takeiri, Plasma Fusion Res. **11**, 2505038 (2016).